Evidence for a short-range chemical order of Ge atoms and its critical role in inducing a giant magnetocaloric effect in $Gd_5Si_{1.5}Ge_{2.5}$

Ronghui Kou[a], Jianrong Gao[a,*], Zhihua Nie[b], Yandong Wang[c], Dennis E. Brown[d], Yang Ren[e]

[a] Key Laboratory of Electromagnetic Processing of Materials (Ministry of Education), Northeastern University, Shenyang 110819, China

[b] College of Materials Science and Engineering, Beijing Institute of Technology, Beijing 100124, China

[c] State Key Laboratory for Advanced Metals and Materials, University of Science and Technology Beijing, Beijing 100083, China

[d] Department of Physics, Northern Illinois University, De Kalb, IL 60115, USA

[e] X-ray Science Division, Advanced Photon Source, Argonne National Laboratory, Argonne, IL 60439, USA

Abstract

Crystal structure and magnetic properties of $Gd_5Si_{1.5}Ge_{2.5}$ and $Gd_{4.9}Zr_{0.1}Si_{1.5}Ge_{2.5}$ were investigated using high-energy X-ray diffraction and magnetic measurements. Results showed that a Zr substitution for 2% Gd reduces unit cell volumes of a room-temperature monoclinic and a low-temperature orthorhombic lattice and a difference between them at a magnetostructural transition. At a microscopic level, the Zr substitution increases length of disconnected interlayer T–T bonds of the monoclinic lattice at the expense of length of connected interlayer T–T bonds (T= Si, Ge). These opposing changes of the interlayer T–T bonds provided evidence for existence of a short-range chemical order of Ge atoms in

lattices of $Gd_5Si_{1.5}Ge_{2.5}$ and its weakening by the Zr substitution. Magnetic measurements revealed that the Zr substitution brings about a change of the magnetic structure and a reduction of a giant magnetocaloric effect of $Gd_5Si_{1.5}Ge_{2.5}$. Based on such structural and magnetic changes due to the Zr substitution, we propose a relation between the short-range chemical order and the total entropy change at the magnetostructural transition. Using this relation, a giant magnetocaloric effect and an annealing effect observed over a wide range of $Gd_5(Si,Ge)_4$ composition can be explained quantitatively.

Keywords: Rare earth compound; crystal structure; magnetocaloric effect; synchrotron radiation; X-ray diffraction.

---

* Corresponding author. E-mail: jgao@mail.neu.edu.cn (J. Gao)

1. Introduction

The magnetic refrigeration technology has aroused much interest because of increasing demand of environmental protection and improvement of energy efficiency [1,2]. In this green technology, a magnetic material is used as the working medium that generates a magnetocaloric effect when moving in or moving out of a magnetic field [3]. Pecharsky et al. discovered a giant magnetocaloric effect (GMCE) in a rare earth compound of $Gd_5Si_2Ge_2$ composition near room temperature in 1997 [4]. This effect was termed giant because the maximum total entropy change observed is about twice as large as that of pure Gd. It was established that the GMCE is due to a field-driven magnetostructural transition of first order from a paramagnetic monoclinic lattice to a ferromagnetic orthorhombic lattice [5]. The two lattices comprise similar layers of Gd_5T_4 units (T = Si and Ge). While only a half of interlayer T–T bonds are connected in the monoclinic lattice, all interlayer T–T bonds are connected in the orthorhombic lattice [6]. The transition depends on the connection of the interlayer T–T bonds, which is enabled by shear movements of atoms [7]. The same transition and the resultant GMCE were observed at $Gd_5(Si,Ge)_4$ composition with varied Ge/Si ratios [8,9]. Tuning of the Ge/Si ratio brings about changes of the peak temperature of the GMCE, which can meet requirement of advanced design of magnetic refrigerators [10]. Theoretical calculations predicted that ferromagnetic interactions can be established in each lattice. They are mediated by a hybridization of 5*d* states of Gd with 3*p* or 4*p* states of T atoms and belong to the Ruderman-Kittel-Kasuya-Yosida (RKKY)-type indirect interactions [11]. Using X-ray magnetic circular dichroism measurements, Haskel et al. verified the hybridization and observed its enhancement across a thermally induced transition in a high magnetic field [12]. They suggested that the interlayer Ge–Ge bonds

play a key role in inducing the GMCE in $Gd_5Si_2Ge_2$, but there was no proof of dominance of the Ge–Ge bonds over other kinds of interlayer T–T bonds. On the other hand, theoretical calculations predicted a difference between the hybridization of Gd 5*d* states with Ge 4*p* sates and their hybridization with Si 3*p* states [13]. This prediction suggested that a chemical order of Ge atoms may affect the GMCE. Although this chemical order was hinted at by observations of an annealing effect on the GMCE [14], it has proven difficult to resolve using X-ray or electron diffraction [10,15,16]. This difficulty is rooted in a small difference between sizes of Ge and Si atoms and a microscopic level of the chemical order. For this difficulty, the formation of the chemical order of Ge atoms and its role in inducing the GMCE are open questions.

As reviewed by Miller [17], many studies have been carried out to investigate effects of chemical substitutions on the structure and magnetism of Gd_5T_4-type tetrelides, aiming at improvement of their GMCEs or at an in-depth understanding of their structure-magnetism relationship. Isoelectric Sn substitutions for T have effects similar to those induced by increasing the Ge/Si ratio of $Gd_5(Si,Ge)_4$ composition [18,19]. In contrast, substitutions of Ga, Sb or P for T can adjust the disconnection of interlayer T–T bonds allowing for thermally induced stabilization of three kinds of lattices and tuning of the ground-state magnetism [20–22]. Substitutions of transition metal for T may have an indirect effect. Of particular interest, partial substitutions of Fe for Ge reduce field hysteresis of the transition at the cost of the GMCE due to formation of impurity phases [23,24]. Substitutions of heavy RE for Gd can preserve the GMCE of $Gd_5Si_2Ge_2$ but reduce the transition temperature severely [25,26]. Substitutions of light RE for Gd leads to formation of spiral magnetism and a reduction of the GMCE [27]. Those effects were interpreted by

considering a lanthanide contraction and a change of anisotropy of RE ions [17,28]. As a new mechanism, a charge transfer of 5*d* electrons was found to occur in Nd-substituted Gd_5Si_4 [29], which tunes ferromagnetism into ferrimagnetism at a high substitution level. Substitutions of non-RE elements for Gd were also investigated. Yao et al. found that partial substitutions of Zr for Gd weaken ferromagnetism of Gd_5Si_4 and may reduce the orthorhombic lattice into a tetragonal one [30]. Those effects were attributed to differences in size and valence electron number between Gd and Zr atoms. Prabahar et al. showed that partial substitutions of Zr for Gd degrade the GMCE by introduction of impurity phases [31]. Up to now, none of studies have provided proofs for promotion or destruction of any chemical order of Ge atoms in lattices of ternary $Gd_5(Si,Ge)_4$ composition.

In this paper, we report experimental proofs of a short-range chemical order of Ge atoms in lattices of $Gd_5Si_{1.5}Ge_{2.5}$ composition. Those proofs were obtained by in situ observations of opposing changes of interlayer T–T bonds induced by a minor Zr substitution for Gd. Furthermore, our observations of an excess reduction of the GMCE due to the Zr substitution hinted at a critical role of the short-range chemical order of Ge atoms in inducing the GMCE. Following such observations, we propose a relation between the population of disconnected Ge–Ge bonds of the monoclinic lattice and a structural entropy change at a field-driven magnetostructural transition. Last, we present that GMCEs and an annealing effect previously observed over a wide range of $Gd_5(Si,Ge)_4$ composition can be quantitatively explained using this relation.

2. Experimental Details

Button-sized ingots of bulk composition $Gd_{5-x}Zr_xSi_{1.5}Ge_{2.5}$ (x = 0 and 0.1) were prepared

by arc-melting Gd (99.9% purity), Zr (99.99% purity), Si and Ge (99.999% purity) in a Ti-gettered argon atmosphere. Each ingot had a mass of about 1 g. An excess mass of 5 wt.% were added for Gd to compensate for losses due to evaporation. The ingots were remelted twice for bulk homogeneity. They were cut into small pieces or pulverized into powders for different measurements. First, differential scanning calorimetric (DSC) measurements were carried out to determine transition temperatures of samples in a zero-field condition. A TA Instrument Q100 calorimeter was used, which provided a temperature accuracy of 0.1 K. The samples were cooled and warmed at a rate of 10 K min^{-1}. Magnetization in the temperature range 50–350 K was measured using a magnetometer fixed in a superconducting quantum interference device. Isothermal magnetization measurements were carried out in d.c. magnetic fields of up to 2 T at temperatures close to Curie temperatures of the samples. High energy X-ray diffraction (HEXRD) measurements were carried out on powder samples using monochromatized synchrotron radiation X-rays with a wavelength of 0.10801 Å at the beamline 11–ID–C of Advanced Photon Source, Argonne National Laboratory. The samples were capsulated into resin-made capillary tubes. They were fixed onto a frame-shaped holder and immersed in a cool bath of liquid nitrogen. They were cooled down 200 K first and warmed up to 290 K. Temperatures of the samples were adjusted by flowing helium into the cool bath and were monitored using a thermal sensor attached to the holder. To reduce a thermal lag between the samples and the holder, the samples were held at each temperature step of 10 K for three minutes. Diffracted X-rays were detected using a two-dimensional amorphous silicon detector with a pixel resolution of 0.2 × 0.2 mm^2 and integrated over each diffraction ring. The detector was placed at a distance of about 2 m away from the samples. The distance was calibrated using

diffraction measurements on a reference sample of CeO_2 at room temperature. Lattice parameters of the samples were determined by Rietveld refinement of integrated diffraction patterns and had errors of the order of 10^{-4}.

3. Results

3.1 DSC measurements

DSC curves of Fig. 1 showed a thermally induced transition for each sample. In cooling, an exothermic peak was observed at 205 and 202 K for the Zr-free and Zr-substituted sample, respectively. In warming, an endothermic peak was observed at 215 and 212 K, respectively. These temperatures suggested a first order nature of the transition and a lowering of the transition temperature by the Zr substitution. As shown below, this transition was determined to be a monoclinic-orthorhombic transition, which is typical in the Gd_5Si_4–Gd_5Ge_4 system [6,8].

3.2 HEXRD measurements

As shown in Figs. 2a and 2b, both samples crystallized into a monoclinic and an orthorhombic lattice at 290 K and 200 K, respectively. These lattices are similar to those proposed for $Gd_5Si_2Ge_2$ [5–7]. In each lattice, T atoms were tentatively assumed to occupy their inequivalent sites randomly. Gd and Zr atoms were assumed to occupy similar sites in terms of respective proportions. Zr atoms were unlikely to occupy T sites because of their weaker electronegativity. As shown in Figs. 2c–2f, residual differences between the observed and calculated HEXRD patterns were smaller than 10%, except for a slightly larger one for the Zr-free sample at the room temperature. Trials assuming preferred occupation of Zr or Ge atoms did not reduce the residual differences further. Nevertheless,

a short-range chemical order of either species could not be ruled out because the Rietveld refinement determined a lattice on a scale of 100 nm or larger. Impurity phases were not identified in either sample. If any existed, its volume fraction would be smaller than a detection limit of 1%. As shown in Fig. 3, temperature-dependent HEXRD measurements confirmed the monoclinic-orthorhombic transition in each sample. In cooling, a diffraction pattern of the Zr-free sample observed at 230 K showed a coexistence of diffraction peaks from the two kinds of lattices. In contrast, patterns observed at other temperatures showed diffraction peaks from one lattice only. In warming, the coexistence of the diffraction peaks from both lattices started at 220 K and ended at 230 K. The starting temperature was 10 K lower than in warming. This anomaly was ascribed to the thermal lag between the samples and the thermal sensor. The thermal lag was larger in cooling than in warming. The structural transition of the Zr-substituted sample set in at 210 K in cooling and warming. The thermal hysteresis of the transition could not be determined because of the use of a temperature step of 10 K. Details of the Rietveld refinement of the HEXRD patterns at each temperature can be obtained from the Fachinformationszentrum Karlsruhe, D-76344 Eggenstein-Leopoldshafen, Germany on quoting depository numbers 1914426−1914465.

As shown in Fig. 4, the lattice parameters of the monoclinic lattice of the Zr-free sample had values of a = 7.604 Å, b = 14.836 Å, c = 7.802 Å, and V = 880.179 Å^3 at 290 K. These parameters are close to those estimated from an extrapolation of the data determined by Pecharsky et al. for composition nearby [6], but show a larger difference relative to the data determined by Choe et al. for the same composition [32]. The larger difference was attributed to formation of a Ge-rich impurity phase, which has been suggested by the latter group but was not evident in the present samples. At 200 K, the lattice parameters of the

orthorhombic lattice had values of a = 7.530 Å, b = 14.818 Å, c =7.808 Å, and V = 871.204 Å^3. Compared to the monoclinic lattice, the orthorhombic lattice had a smaller unit cell volume, which agrees well with previous studies [5–7, 32]. The lattice parameters of the monoclinic lattice of the Zr-substituted sample had values of a = 7.572 Å, b = 14.794 Å, c = 7.800 Å, and V = 873.784 Å^3 at 290 K. The lattice parameters of orthorhombic lattice had values of a = 7.511 Å, b = 14.774 Å, c = 7.802 Å, and V = 865.795 Å^3 at 200 K. These values are smaller than those of the Zr-free sample at similar temperatures, suggesting significant lattice contractions due to the Zr substitution. At 290 K, the monoclinic lattice had a volumetric contraction of $\Delta V/V$ = 0.73%. This contraction is 18% larger than a contraction of $\Delta V/V$ = 0.62% of the orthorhombic lattice at 200 K. The lattice contractions were anisotropic. While the largest contraction of 0.42% was observed along the a axis of the monoclinic lattice, the largest contraction of 0.30% was observed along the b axis of the orthorhombic lattice. The lattice parameters of both samples showed linear changes with declining temperature. At the structural transition, the parameter c showed an increase in contrast to a reduction of other parameters. Despite such opposing changes, the lattices of the Zr-substituted sample had a volumetric contraction of $\Delta V/V$ = 0.63%. This value is 43% larger than a volumetric contraction of $\Delta V/V$ = 0.44% induced by the Zr substitution. In warming, the lattice parameters of the samples were similar to those in cooling and are not shown in Fig. 4.

As shown in Fig. 5, the Zr substitution brought about stronger effects on T–T and Gd–T bonds than on Gd–Gd bonds of the monoclinic lattice. It increased length of interlayer T_{1a}–T_{1a} bonds whereas it reduced length of interlayer T_{1b}–T_{1b} bonds and intralayer T_2–T_3 bonds. These opposing changes of the length of the interlayer T–T bonds suggested that the Zr

substitution had reduced shear movement of T atoms at the structural transition and thus, weakened the first order nature of the transition. For the orthorhombic lattice, the Zr substitution reduced length of interlayer T_1–T_1 bonds more than it reduced length of intralayer T_2–T_3 bonds. It reduced length of interlayer Gd_3–$T_{1a/1b}$ bonds and Gd–Gd bonds of each lattice as well. Despite such a variety, the changes of bond length due to the Zr substitution are small compared to those observed at the thermally induced structural transition.

3.3 Magnetic measurements

Fig. 6 shows temperature dependence of magnetization of the samples at a low and a high magnetic field. A steep rise of magnetization with declining temperature for each sample suggested establishment of a ferromagnetic order. In the low magnetic field, the Zr-free sample showed higher magnetization in warming than in cooling. This difference might be due to alignment of the sample along the magnetic field. The magnetization of the Zr-free sample also showed a two-step decrease. A decrease observed in a second step is much steeper than in an initial step. There is a dip between the steps. The two-step decrease of magnetization suggested two magnetic transitions in warming in contrast to a single transition in cooling. The magnetic transition in cooling was observed at a Curie temperature of 213 K. In terms of the HEXRD measurements, the two transitions in warming were attributed to magnetic ordering of the orthorhombic and the monoclinic lattice, respectively. The single transition in cooling was attributed to a magnetostructural transition, i.e. the two magnetic transitions observed in warming were merged with the structural transition. The magnetostructural transition was evident in the high magnetic field. A Curie temperature of 221 K was observed in warming, which is 6 K higher than a

Curie temperature in cooling. These Curie temperatures suggested positive hysteresis, which is consistent with the first order nature of the magnetostructural transition [5]. A mean Curie temperature of 218 K is 5 K higher than that in the low magnetic field. This difference was due to an improved stability of the ferromagnetic lattice at the higher magnetic field [33]. Magnetization of the Zr-substituted sample also suggested two magnetic transitions in the low magnetic field. They were hinted at by a twist-like discontinuity of magnetization and were discerned more clearly in a plot of the temperature derivative of magnetization (see the inset of Fig. 6c). Their Curie temperatures in cooling are 3 K lower and higher than those in warming, respectively. A transition with the higher Curie temperature was attributed to ferromagnetic ordering of the monoclinic lattice, whereas the other one with the lower temperature was attributed to ferromagnetic ordering of the orthorhombic lattice [11]. In the high magnetic field, the two magnetic transitions were merged into a magnetostructural transition. The merged transition was observed at 218 K and 220 K in cooling and warming, respectively. Its thermal hysteresis is smaller than that of the Zr-free sample, suggesting a weakening of the magnetostructural transition by the Zr substitution.

As shown in Fig. 7, temperature dependence of reciprocal magnetic susceptibility of the samples showed deviations from a Curie-Weiss law. The deviations suggested a Griffiths phase, which is generally attributed to short-range ferromagnetic interactions in a paramagnet [34]. This Griffiths phase is similar to that observed by Ouyang [35]. In the magnetic field of 0.02 T, the Griffiths phase of the Zr-free sample set in at a temperature of 284 K and 281 K in cooling and warming, respectively. Such onset temperatures were reduced to 218 K and 227 K in the magnetic field of 2 T, respectively. This reduction

suggested a weakening of short-range ferromagnetic interactions by the higher magnetic field. The Griffiths phase of the Zr-substituted sample showed a few changes relative to the Zr-free sample. As shown in Figs. 7c and 7d, the onset temperatures were similar in cooling and warming but were less sensitive to the magnetic field. They were reduced by the high magnetic field. A reduction of 11 K is smaller than a mean reduction of 60 K for the Zr-free sample. Such differences suggested that the Zr substitution had reduced both the strength and the field sensitivity of short-range ferromagnetic interactions in a paramagnetic state. A paramagnetic Curie temperature of neither sample was sensitive to the magnetic fields. It did not show any significant irreversibility in warming.

As shown in Figs. 8a and 8b, isothermal magnetization of each sample showed a field-driven metamagnetic transition near respective Curie temperature. This transition could be identified as a magnetostructural transition following a previous study [33]. Compared to the Zr-free sample, the Zr-substituted sample showed a less sharp transition and low magnetization. These differences gave a hint at establishment of a ferrimagnetic structure as discussed in Section 4.2. Fig. 8c shows the total entropy changes of the samples at a magnetic field change from 0 to 2 T. They were determined using the Maxwell relationship [36] and included non-magnetic contributions as explained in Section 4.3. The total entropy change of the Zr-free sample reached a maximum of 16.26 J kg^{-1} K^{-1} at 212.5 K. This value is comparable to a maximum of ~14 J kg^{-1} K^{-1} observed for $Gd_5Si_2Ge_2$ and is by a factor of 2 larger than that of pure Gd [4]. Thus, it could also be termed as a GMCE. An integration of entropy changes larger than a half of the maximum defined a refrigeration capacity power (RCP) of 239 J kg^{-1}. The physical meaning of this quantity was explained elsewhere [37]. The total entropy change of the Zr-substituted sample reached a maximum of 8.16 J

kg^{-1} K^{-1} at 222.5 K. This maximum is roughly a half of the maximum of the Zr-free sample, suggesting a reduction of the GMCE by the Zr substitution. However, it is still larger than that of pure Gd. The Zr-substituted sample was determined to have a RCP of 172 J kg^{-1}, which is smaller than that of the Zr-free sample. The RCP was reduced by the Zr substitution less than the maximum of the total entropy change. The reason is that the Zr substitution brought about a sharp change of high-field magnetization over a wider range of temperature (16 K vs 12 K).

4. Discussion

4.1 Effect on chemical order of lattices

The HEXRD measurements unveiled significant lattice contractions due to the Zr substitution. The contractions can be understood qualitatively in terms of a size difference of 10% between Zr and Gd atoms. However, the volumetric contraction of the monoclinic lattice is 11% larger than that expected at the 2% substitution level. In addition, a 0.42% reduction of the parameter *a* of the monoclinic lattice is 91% larger than an estimated reduction by 0.22%. Such excess lattice contractions can neither be explained by considering the errors of the HEXRD measurements nor by considering those of the Rietveld refinement. Consideration of impurity phases cannot provide a reasonable explanation either because of insufficient volume fractions. We show below that the excess lattice contractions can be explained by considering a weakening of a short-range chemical order by the Zr substitution.

The Rietveld refinement revealed strong effects of the Zr substitution on the bond lengths of the monoclinic lattice. These effects provided proofs of a short-range chemical

order in the lattice of the Zr-free sample and its reduction by the Zr substitution. As shown in Fig. 5, the length of the T–T bonds of the Zr-substituted sample showed the largest changes due to the Zr substitution. This observation suggested a close relation of the lattice contractions with the changes of interlayer T–T bonds. Because Ge atoms are larger than Si atoms, an increase of the length of the connected interlayer T_{1a}–T_{1a} bonds requires an increase of the population of Ge atoms. On the contrary, a decrease of the length of the disconnected interlayer T_{1b}–T_{1b} bonds requires a decrease of the population of Ge atoms. To satisfy these opposing requirements, Ge and Si atoms are supposed to distribute themselves more homogenously in the lattice of the Zr-substituted sample. This more homogeneous redistribution inversely suggested a less homogeneous distribution of the same species in the lattice of the Zr-free sample and thus, provided evidence for the existence of a short-range chemical order. As illustrated in Fig. 9, the short-range chemical order is most likely characterized by a layer-by-layer distribution of disconnected interlayer Ge–Ge bonds and connected interlayer Si–Si bonds in the middle $Gd_5Si_2Ge_2$ composition. In Ge-rich composition, interlayer Si–Si bonds may be partially or completely replaced by interlayer Si–Ge bonds, which are supposed to be connected. In Si-rich composition, disconnected interlayer Ge–Ge bonds may be partially replaced by the connected Si–Ge bonds. For such replacement, the short-range chemical order of Ge atoms is supposed to be weakened in lattices of off-middle composition. In the Zr-substituted sample, the short-range chemical order is significantly reduced due to the redistribution of Ge atoms. This reduction is most likely to be driven by a rebalance of microscopic lattice strains. Although tendencies in site occupation of Zr or Ge atoms could not be resolved by the Rietveld refinement, the changes of the order of 10^{-3} of bond length were large enough to be resolved.

The disconnected and connected interlayer T–T bonds are supposed to bear microscopic strains of opposite signs: tensile strains on the short and connected T_{1a}–T_{1a} bonds and compressive strains on the long and disconnected T_{1b}–T_{1b} bonds. There should be a microscopic balance between these strains in order to minimize the total strain energy. The local balance may be broken upon the Zr substitution for Gd because of formation of Zr–T bonds. The Zr–T bands are shorter than the Gd–T bonds and can impose tensile strains on neighboring Gd–T bonds. To balance such strains, a large amount of Ge atoms are "forced" to occupy T_1 sites where connected interlayer T_{1a}–T_{1a} bonds are formed. Meanwhile, an equivalent amount of Si atoms are "pushed" back to T_1 sites where disconnected interlayer T_{1b}–T_{1b} bonds are formed. This redistribution of T atoms brings about enhancement of the mean 5*d*–4*p*/3*p* hybridization and helps stabilize the Gd(Zr)–T bonds. The stabilization effect was suggested by the observation of the reduction of the length of Gd_3–$T_{1a/1b}$ bonds (see Fig. 5c). Because the structural transition does not require diffusion of any atoms, the short-range chemical order of the monoclinic lattice is supposed to exist also in the orthorhombic lattice. The chemical order can lower the total strain energy and therefore helps stabilize both lattices. The larger contraction of the monoclinic lattice due to the Zr substitution suggested a larger reduction of the lattice strain energy and therefore a larger increase of its lattice stability. This hypothesis is consistent with the observation of the lowered transition temperature for the Zr-substituted sample (see Fig. 1). Thus, the role of microscopic lattice strains in forming or reducing the short-range chemical order of Ge atoms is justified.

4.2 Effect on magnetism

The magnetic measurements showed an increase of the Curie temperature at the cost of

magnetization due to the Zr substitution. These observations suggested a possible change of magnetism in the orthorhombic lattice. Because of strong absorption of neutrons by Gd atoms, it is difficult to check this possibility using neutron diffraction. To bypass this difficulty, we turn to a quantitative analysis of temperature and field dependence of magnetization of the samples. The data of Fig. 8 suggested a reduction of isothermal magnetization due to the Zr substitution. However, the reduction is much larger than a reduction due to a magnetic dilution. There should be other reasons for the excess reduction. The less sharp metamagnetic transition provided a clue for a coexistence of ferromagnetic and antiferromagnetic interactions in the lattice. This coexistence means that the Zr substitution stabilizes a ferrimagnetic structure against a ferromagnetic one. The antiferromagnetic interactions are supposed to be arise from the weakening of the short-range chemical order of the monoclinic lattice. Due to the more homogeneous distribution of T atoms in the lattices, locally disconnected Ge–Ge bonds can easily find neighbors of the same species. Thus, there are Si-free segments. Despite a small volume fraction, those segments are dominated by the disconnected interlayer Ge–Ge bonds thus allowing for development of antiferromagnetic interactions similar to those favored in binary Gd_5Ge_4 [38]. The hypothesis of the ferrimagnetic structure can immediately account for the excess reduction of magnetization by considering cancellation of moments of local Gd atoms by a factor of 2. It can also provide self-consistent explanations of the weaker Griffiths phase and its high-field sensitivity. Its extension to lower temperatures via the magnetostructural transition can account for the diminishing difference between magnetization of the high-temperature and low-temperature lattices.

The Curie temperature of a ferromagnet is determined by its spin-polarized electronic

structure at the Fermi surface [12,39]. Each Zr atom carries two 5*d* electrons whereas each Gd atom carries only one. Thus, the Zr substitution may bring about a charge transfer as has been observed for Nd substitution for Gd in Gd_5Si_4 [29]. Then the charge transfer is supposed to induce a change of the electronic structure at the Fermi surface because of a change of the bond length-dependent 5*d*–3*p*/4*p* hybridization [12]. From this point of view, the effect of the Zr substitution on the Curie temperature is similar to that of hydrostatic pressures. Tseng et al. determined that the Curie temperatures of $Gd_5Si_2Ge_2$ increases linearly with rising pressure up to 10 GPa [40]. On the other hand, Svitelskiy et al. determined a bulk modulus of 68.5 GPa for $Gd_5Si_2Ge_2$ [41]. Assuming that this bulk modulus is true also for the present samples and does not depend on temperature, creation of the 0.73% volumetric contraction requires a hydrostatic pressure of 0.5 GPa. At this pressure, the Curie temperature is estimated to be raised by 6 K in terms of a linear pressure coefficient of 12 K/GPa [40]. This estimation agrees well with the observations on the Curie temperature of the present samples at the low magnetic field. On the other hand, a decrease of the Curie temperature by 1 K at the high magnetic field of 2 T can be understood by considering field-induced instability of the antiferromagnetic interactions.

4.3 Role of interlayer Ge–Ge bonds in inducing GMCE

A magnetocaloric effect due to a magnetic transition of a ferromagnet usually comprises a magnetic entropy change, an electronic entropy change and a lattice entropy change [42,43]. These ingredients were also included in the magnetocaloric effect of the present samples. The lattice entropy change was due to losses of vibration of the disconnected interlayer T_{1b}–T_{1b} bonds of the monoclinic lattice at the structural transition. The electronic entropy change was due to the enhancement of the 5*d*–3*p*/4*p* hybridization at the structural

transition. A sum of them can be termed a structural entropy change following Gschneidner Jr. et al. [42]. As explained by von Ranke et al. [44], the total entropy changes observed at a first order magnetic transition can be calculated using the Maxwell relationship. Because magnetization often changes insignificantly over a small temperature window, the Maxwell relationship can be simplified as a linear relation between the isothermal magnetic entropy change and a change in magnetization. Using this simplified relationship, the effect of the Zr substitution on the magnetic and the structural entropy change at the field-driven transition can be analyzed quantitatively. As suggested above, the reduction of magnetization of the Zr-substituted sample was due to antiferromagnetic interactions between local Gd atoms and the magnetic dilution. To determine this reduction accurately, magnetization of the samples observed at lower temperatures are extrapolated towards a temperature, where the total entropy changes reached their maxima. A value of 88.9 emu g^{-1} is determined for Zr-substituted sample, which is 15.3% lower than a value of 104.9 emu g^{-1} for the Zr-free sample. This total reduction of magnetization comprises a 2% reduction due to the magnetic dilution and a 13.3% excess reduction due to the antiferromagnetic interactions. As explained in Section 4.2, the excess reduction requires an increase of the population of the disconnected interlayer Ge–Ge bonds by 6.6%, which is the very reason for a 35.0% reduction of the structural entropy change. In terms of such a relation, the structure entropy change is estimated to have an absolute reduction of 0.87 J mol^{-1} K^{-1} per percentage decrease of the population of the disconnected interlayer Ge–Ge bonds. Reversely, the structural entropy change of the Zr-free sample is estimated to gain an increase of the same amount. For this large increase, the GMCE at the field-driven transition can be enhanced by an increase of the population of the disconnected Ge–Ge

bonds. Technically, the population of the disconnected Ge–Ge bonds can be enlarged by raising Ge concentration or by annealing of as-cast composition. Such chemical and annealing effects were already observed in previous studies [8,9,14]. We present below a quantitative explanation of GMCEs observed over a wide range of $Gd_5(Si,Ge)_4$ composition.

For convenience, we rewrite the chemical formula $Gd_5(Si,Ge)_4$ as $Gd_5Si_{4-y}Ge_y$, where y = 0–4. For a given y, a percentage of the population of disconnected interlayer Ge–Ge bonds, P, out of the total population of T–T bonds of a monoclinic lattice can be expressed as

$$P = y \times 100 /4/2 = 12.5y = 25\ (\%)\ . \quad (1)$$

When these Ge–Ge bonds are connected at a field-driven transition, they will bring about a structural entropy change

$$\Delta S_{str.} = 0.87 \times P\ = 10.875\ y\ (J\ mol^{-1}\ K^{-1}). \quad (2)$$

We assume that a magnetic entropy change, $\Delta S_{mag.}$, is independent of y and has an absolute magnitude of 5.0 J mol^{-1} K^{-1} at a magnetic field change from 0 to 2 T. This value is slightly larger than a value of 4.2 J mol^{-1} K^{-1} observed on Gd_5Si_4 [45], but it can provide a reasonable explanation of the GMCE of $Gd_5Si_2Ge_2$. Under such assumptions, a maximum of the total entropy change can be expressed as

$$\Delta S_{tot.} = \Delta S_{mag.} + \Delta S_{str.} = 10.875\ y + 5.0\ (J\ mol^{-1}\ K^{-1}). \quad (3)$$

This maximum of the total entropy change can be converted into its value in J kg^{-1} K^{-1} by dividing the right-hand term of Eq. (3) by a molar mass, M, namely

$$\Delta S_{tot.} = (10.875\ y + 5.0)/M\ (J\ kg^{-1}\ K^{-1}). \quad (4)$$

Substituting M = 0.988 kg mol^{-1} and y = 2 into Equation (4), we obtain a maximum of the

total entropy change of 27.1 J kg^{-1} K^{-1} for $Gd_5Si_2Ge_2$ at a magnetic field change from 0 T to 2 T. This value agrees well with an observed value of 27.0 J kg^{-1} K^{-1} [14]. Assuming that the magnetic entropy change scales with the magnetic field change, it should have a value of 12.5 J mol^{-1} K^{-1} at a magnetic field change from 0 to 5 T. Then the maximum of the total entropy change is given by

$$\Delta S_{tot.} = (10.875\ y + 12.5)/M\ (J\ kg^{-1}\ K^{-1}). \quad (5)$$

Using Eq. (5), we predict a maximum of the total entropy change of 34.7 J kg^{-1} K^{-1} for $Gd_5Si_2Ge_2$ at a magnetic field change from 0 to 5 T. This predicted value again agrees well with an observed value of 36. 4 J kg^{-1} K^{-1} [14]. Such agreements suggest that the assumptions made above are reasonable. A larger total entropy change can be accessed by Ge-rich composition provided that interlayer and intralayer Ge–Ge bonds of its monoclinic lattice play similar roles and get connected at the field-driven transition. For the Ge-rich $Gd_5Si_{1.5}Ge_{2.5}$, its total entropy change at a magnetic field change from 0 to 2 T is predicted to have a maximum of 31.9 J kg^{-1} K^{-1}. This predicted value is nearly doubled relative to a value of 16.26 J kg^{-1} K^{-1} observed for the Zr-free sample. A large difference can be attributed to a smaller population of the disconnected interlayer Ge–Ge bonds than the theoretical maximum given by Eq. (1) at y = 2.5. Annealing may help improve the GMCE by accessing the maximum population of the disconnected Ge–Ge bonds. This speculation is verified by a close agreement between a predicted maximum of 39.3 J kg^{-1} K^{-1} and an observed maximum of 43.9 J kg^{-1} K^{-1} at a magnetic field from 0 to 5 T [9]. As listed in Table 1, the predicted maxima of the total entropy changes over a wide range of $Gd_5Si_{4-y}Ge_y$ composition show a fairly good agreement with previous observations [9,14] within an accuracy of 12%. Larger discrepancies at Ge-richer or Si-richer composition can

be attributed to enhanced antiferromagnetic interactions or experimental difficulty in maximization of the population of the disconnected Ge–Ge bonds by annealing. Despite such discrepancies, the general agreement between the predictions and the observations confirms that the disconnected Ge–Ge bonds play a critical role in inducing a GMCE in all of those composition.

5. Conclusions

The present study has revealed significant effects of the minor Zr substitution for Gd on the lattice parameters, bond length, magnetization and GMCE of $Gd_5Si_{1.5}Ge_{2.5}$. The Zr substitution preserves a first order magnetostructural transition but brings about opposing changes of the length of disconnected and connected interlayer T–T bonds (T= Si and Ge). Such changes have provided first evidence for a short-range chemical order of Ge atoms in the lattices of $Gd_5Si_{1.5}Ge_{2.5}$ and a reduction of it by the Zr substitution. Observations of an excess reduction of magnetization beyond a magnetic dilution effect have suggested stabilization of ferrimagnetism by the Zr substitution. The ferrimagnetism has been related to the reduction of the short-range chemical order. Such a structure-magnetism relationship has allowed for a quantitative evaluation of the structural entropy change at a field-driven magnetostructural transition. The maxima of the total entropy changes of a series of $Gd_5(Si,Ge)_4$ composition have been predicted in terms of a maximum of the population of disconnected Ge–Ge bonds in their monoclinic lattices. The predictions have shown a general agreement with previous observations [9,14], thus confirming a critical role of disconnected Ge–Ge bonds in inducing their GMCEs.

Acknowledgements

This work was supported by the National Natural Science Foundation of China [grant number 51831003]; the Ministry of Science and Technology of China [grant number 2012CB619405]. The authors thank S. Guo, A. Yan, J. Q. Wang and S. Yang for assistance in magnetic measurements. This research used resources of the Advanced Photon Source, a U.S. Department of Energy (DOE) Office of Science User Facility operated for the DOE Office of Science by Argonne National Laboratory under Contract No. DE-AC02-06CH11357.

References

[1] A. Smith, C. R. H. Bahl, R. Bjørk, K. Engelbrecht, K. K. Nielsen, N. Pryds, Materials challenges for high performance magnetocaloric refrigeration devices, Adv. Energy Mater. 2 (2012) 1288–1318. https://doi.org/10.1002/aenm.201200167.

[2] D. Y. Cong, L. Huang, V. Hardy, D. Bourgault, X. M. Sun, Z. H. Nie, M. G. Wang, Y. Ren, P. Ental, Y. D. Wang, Low-field-actuated giant magnetocaloric effedt and excellent mechanical properties in a NiMn–based multiferroic alloy, Acta Mater. (2018) 142–151. https://doi.org/10.1016/j.actamat.2017.12.047.

[3] N. H. Dung, Z. Q. Ou, L. Caron, L. Zhang, D. T. Cam Thanh, G. A. de Wijs, R. A. de Groot, K. H. J. Buschow, E. Brück, Mixed magnetism for refrigeration and energy conversion, Adv. Energy Mater. 1 (2011) 1215–1219. https://doi.org/10.1002/aenm.201100252.

[4] V. K. Pecharsky, K. A. Gschneidner Jr., Giant magnetocaloric effect in $Gd_5(Si_2Ge_2)$, Phys. Rev. Lett. 78 (1997) 4494–4497. https://doi.org/10.1103/PhysRevLett.78.4494.

[5] V. K. Pecharsky, K. A. Gschneidner Jr., $Gd_5(Si_xGe_{1-x})_4$: an extremum material, Adv. Mater. 13 (2001) 683–686. https://doi.org/10.1002/1521-4095(200105)13:9.

[6] V. K. Pecharsky, K. A. Gschneidner Jr., Phase relationships and crystallography in the pseudobinary system Gd_5Si_4–Gd_5Ge_4, J. Alloys Compd. 260 (1997) 98–106. https://doi.org/10.1016/S0925-8388(97)00143-6.

[7] W. Choe, V. K. Pecharsky, A. O. Pecharsky, K. A. Gschneidner Jr., V. G.Young Jr., G. J. Miller, Making and breaking covalent bonds across the magnetic transition in the giant magnetocaloric material $Gd_5(Si_2Ge_2)$, Phys. Rev. Lett. 84 (2000) 4617–4620. https://doi.org/10.1103/PhysRevLett.84.4617.

[8] V. K. Pecharsky, K. A. Gschneidner Jr., Tunable magnetic regenerator alloys with a giant magnetocaloric effect for magnetic refrigeration from ~20 to ~290 K, Appl. Phys. Lett. 70 (1997) 3299–3301. https://doi.org/10.1063/1.119206.

[9] K. A. Gschneidner Jr., V. K. Pecharsky, A. O. Tosol, Recent developments in magnetocaloric materials, Rep. Prog. Phys. 68 (2005) 1479–1539. https://doi.org/10.1088/0034-4885/68/6/R04.

[10] J. A. Barclay, Active and passive magnetic regenerators in gas/magnetic refrigerators, J. Alloys Compd. 207 (1994) 355–361. https://doi.org/10.1016/0925-8388(94)90239-9.

[11] D. Paudyal, V. K. Pecharsky, K. A. Gschneidner Jr., B. Harmon, Electron correlation effects on the magnetostructural transition and magnetocaloric effect in $Gd_5Si_2Ge_2$, Phys. Rev. B 73 (2006) 144406. https://doi.org/10.1103/PhysRevB.73.144406.

[12] D. Haskel, Y. B. Lee, B. N. Harmon, Z. Islam, J. C. Lang, G. Srajer, Ya. Mudryk, K. A. Gschneidner Jr., V. K. Percharsky, Role of Ge in bridging ferromagnetism in the

giant magnetocaloric $Gd_5(Ge_{1-x}Si_x)_4$ alloys, Phys. Rev. Lett. 98 (2007) 247205. https://doi.org/10.1103/PhysRevLett.98.247205.

[13] G. Skorek, J. Deniszczyk, J. Szade, Electronic structure of $Gd_5(Si,Ge)_4$, J. Phys.: Condens. Matter 14 (2002) 7273−7286. https://doi.org/10.1088/0953-8984/14/30/316.

[14] A. O. Pecharsky, K. A. Gschneidner Jr., V. K. Pecharsky, The giant magnetocaloric effect of optimally prepared $Gd_5Si_2Ge_2$, J. Appl. Phys. 93 (2003) 4722–4728. https://doi.org/10.1063/1.1558210.

[15] J. S. Meyers, S. Chumbley, F. Laabs, A. O. Percharsky, TEM analysis of $Gd_5(Si_xGe_{1-x})_4$, where x=1/2, Acta Mater. 51 (2003) 61–70. https://doi.org/10.1016/S1359-6454(02)00227-6.

[16] V. K. Pecharsky, G. D. Samolyuk, V. P. Antropov, A. O. Pecharsky, K. A. Gschneidner Jr., The effect of varying the crystal structure on the magnetism, electronic structure and thermodynamics in the $Gd_5(Si_xGe_{1-x})_4$ system near x= 0.5, J. Solid State Chem. 171 (2003) 57–68. https://doi.org/10.1016/S0022-4596(02)00146-9.

[17] G. J. Miller, Complex rare-earth tetrelides, $RE_5(Si_xGe_{1-x})_4$: new materials for magnetic refrigeration and a superb playground for solid state chemistry, Chem. Soc. Rev. 35 (2006) 799–813. https://doi.org/10.1039/B208133B.

[18] H. B. Wang, Z. Altounian, D. H. Ryan, Structural and magnetic properties of $Gd_5Si_xSn_{4-x}$, Phys. Rev. B 66 (2002)214413. https://doi.org/10.1103/PhysRevB.66.214413.

[19] A. M. G. Carvalho, J. C. G. Tedesco, M. J. M. Pires, M. E. Soffner, A. O. Guimarães, A. M. Mansanares, A. A. Coelho, Large magnetocaloric effect and refrigerant capacity near room temperature in as-cast $Gd_5Ge_2Si_{2-x}Sn_x$ compounds, Appl. Phys. Lett. 102 (2013) 192410. https://doi.org/10.1063/1.4806971.

[20] Y. Mozharivskyj, W. Choe, A. O. Pecharsky, G. J. Miller, Phase transformation driven by valence electron concentration: tuning interslab bond distances in $Gd_5Ga_xGe_{4-x}$, J. Am. Chem. Soc. 125 (2003) 15183–15190. https://doi.org/10.1021/ja037649z.

[21] V. Svitly, G. J. Miller, Y. Mozharivskyj, $Gd_5Si_{4-x}P_x$: targeted structural changes through increase in valence electron count, J. Am. Chem. Soc. 131 (2009) 2367–2374. https://doi.org/10.1021/ja8085033.

[22] J. Yao, Y. Zhang, P. L. Wang, L. Lutz, G. J. Miller, Y. Mozharivskyj, Electronically induced ferromagnetic transitions in Sm_5Ge_4–type magnetoresponsive phases, Phys. Rev. Lett. 110 (2013) 077204. https://doi.org/10.1103/PhysRevLett.110.077204.

[23] V. Provenzano, A. J. Shapiro, R. D. Shull, Reduction of hysteresis losses in the magnetic refrigerant $Gd_5Ge_2Si_2$ by the addition of iron, Nature 429 (2004) 853. https://doi.org/10.1038/nature02657.

[24] D. M. Raj Kumar, M. Manivel Raja, R. Gopalan, A. Sambasiva Rao, V. Chandrasekaran, Effect of Fe-substitution on microstructure, hysteresis behavior and magnetocaloric effect in $Gd_5Si_2Ge_2$ Alloys, J. Magn. Magn. Mater. 321 (2009) 1300–1305. https://doi.org/10.1016/j.jmmm.2008.11.094.

[25] K. A. Gschneidner Jr., V. K. Pecharsky, A. O. Pecharsky, V. V. Ivtchenko, E. M. Levin, The nonpareil $R_5(Si_xGe_{1-x})_4$ phases, J. Alloys Compd. 303 (2000) 214–222. https://doi.org/10.1016/S0925-8388(00)00747-7.

[26] Z. W. Ouyang, G. H. Rao, Crystal structures, phase relationships, and magnetic phase transitions of R_5M_4 compounds (R= rare earths, M= Si, Ge), Chin. Phys. B 22.9 (2013) 097501. https://doi.org/10.1088/1674-1056/22/9/097501.

[27] C. Magen, C. Ritter, L. Morellon, P. A. Algarabel, M. R. Ibarra, Magnetic ordering in

the monoclinic structure of $Nd_5Si_{1.45}Ge_{2.55}$ and $Pr_5Si_{1.5}Ge_{2.5}$ studied by means of neutron powder diffraction, J. Phys.: Condens. Matter 16 (2004) 7427–7437. https://doi.org/10.1088/0953-8984/16/41/022.

[28] K. A. Gschneidner Jr., The magnetocaloric effect, magnetic refrigeration and ductile intermetallic compounds, Acta Mater. 57 (2009) 18–28. https://doi.org/10.1016/j.actamat.2008.08.048.

[29] R. H. Kou, J. Gao, Y. Ren, B. Sanyal, S. Bhandary, S. M. Heald, B. Fisher, C. -J. Sun, Charge transfer-tuned magnetism in Nd-substituted Gd_5Si_4, AIP Adv. 8 (2018) 125219. https://doi.org/10.1063/1.5081457.

[30] J. Yao, Y. Mozharivskyj, Site preference of metal atoms in $Gd_{5-x}M_xTt_4$ (M= Zr, Hf; Tt= Si, Ge), Z. Anorg. Allg. Chem. 637 (2011) 2039–2045. https://doi.org/10.1002/zaac.201100281.

[31] K. Prabahar, D. M. Raj Kumar, M. Manivel Raja, V. Chandrasekaran, Phase analysis and magnetocaloric properties of Zr substituted Gd–Si–Ge alloys, J. Magn. Magn. Mater. 323 (2011) 1755–1759. https://doi.org/10.1016/j.jmmm.2011.01.029.

[32] W. Choe, G. J. Miller, J. Meyers, S. Chumbley, A. O. Pecharsky, “Nanoscale zippers” in the crystalline solid. structural variations in the giant magnetocaloric material $Gd_5Si_{1.5}Ge_{2.5}$, Chem. Mater. 15 (2003) 1413–1419. https://doi.org/10.1021/cm020928l.

[33] F. Casanova, A. Labarta, X. Batlle, J. Marcos, L. Manosa, A. Planes, S. de Brion, Effect of a magnetic field on the magnetostructural phase transition in $Gd_5(Si_xGe_{1-x})_4$, Phys. Rev. B 69 (2004) 104416. https://doi.org/10.1103/PhysRevB.69.104416.

[34] M. Zou, V. K. Pecharsky, K. A. Gschneidner Jr., D. L. Schlagel, T. A. Lograsso,

Magnetic phase transitions and ferromagnetic short-range correlations in single-crystal $Tb_5Si_{2.2}Ge_{1.8}$, Phys. Rev. B 78 (2008) 014435. https://doi.org/10.1103/PhysRevB.78.014435.

[35] Z. W. Ouyang, Griffiths-like behavior in Ge-rich magnetocaloric compounds $Gd_5(Si_xGe_{1-x})_4$, J. Appl. Phys. 108 (2010) 033907. https://doi.org/10.1063/1.3467800.

[36] J. S. Amaral, N. J. O. Silva, V. S. Amaral, Estimating spontaneous magnetization from a mean field analysis of the magnetic entropy change, J. Magn. Magn. Mater. 322 (2010) 1569–1571. https://doi.org/10.1016/j.jmmm.2009.09.024.

[37] V. K. Pecharsky, K. A. Gschneidner Jr, Some common misconceptions concerning magnetic refrigerant materials, J. Appl. Phys. 90 (2001) 4614–4622. https://doi.org/10.1063/1.1405836.

[38] C. Magen, Z. Arnold, L. Morellon, Y. Skorokhod, P. A. Algarabel, M. R. Ibarra, J. Kamarad, Pressure-induced three-dimensional ferromagnetic correlations in the giant magnetocaloric compound Gd_5Ge_4, Phys. Rev. Lett. 91 (2003) 207202. https://doi.org/10.1103/PhysRevLett.91.207202.

[39] P. Mohn, E. P. Wohlfath, The Curie temperature of the ferromagnetic transition metals and their compounds, J. Phys. F: Met. Phys. 17 (1987) 2421. https://doi.org/10.1088/0305-4608/17/12/016.

[40] Y. C. Tseng, D. Haskel, J. C. Lang, S. Sinogeikin, Ya. Mudryk, V. K. Pecharsky, K. A. Gschneidner Jr., Effect of hydrostatic pressure upon the magentic transitions in the $Gd_5(Si_xGe_{1-x})_4$ compounds: X-ray magnetic circular dichroism study, Phys. Rev. B 76 (2007) 014401. https://doi.org/10.1103/PhysRevB.76.014401.

[41] O. Svitelskiy, A. Suslov, D. L. Schlagel, T. A. Lograsso, K. A. Gschneidner Jr., V. K.

Percharsky, Elastic properties of $Gd_5Si_2Ge_2$ studied with an ultrasonic pulse-echo technique, Phys. Rev. B 74 (2006) 184105. https://doi.org/10.1103/PhysRevB.74.184105.

[42] A. M. Tishin, Magnetocaloric effect in strong magnetic fields, Cryogenics 30 (1990) 127–136. https://doi.org/10.1016/0011-2275(90)90258-E.

[43] K. A. Gschneidner Jr, Y. Mudryk, V. K. Pecharsky, On the nature of the magnetocaloric effect of the first order magnetostructural transition, Scrip. Mater. 67 (2012) 572–577. https://doi.org/10.1016/j.scriptamat.2011.12.042.

[44] P. J. von Ranke, N. A. de Oliverira, C. Mello, A. M. G. Carvalho, S. Gama, Analytical model to understand the colossal magnetocaloric effect, Phys. Rev. B 71 (2005) 054410. https://doi.org/10.1103/PhysRevB.71.054410.

[45] Y. I. Spichkin, V. K. Pecharsky, K. A. Gschneidner Jr., Preparation, crystal structure, magnetic and magnetothermal properties of $(Gd_xR_{5-x})Si_4$, where R=Pr and Tb, alloys, J. Appl. Phys. 89 (2001) 1738–1745. https://doi.org/10.1063/1.1335821.

List of Tables

Table 1 Comparison of previously measured and predicted total entropy changes of $Gd_5(Si,Ge)_4$ composition at a magnetic field change from 0 to 5 T. Measured data are taken from Refs. [9,14].

Bulk composition	Observed total entropy change ($J\ kg^{-1}\ K^{-1}$)	Predicted total entropy change ($J\ kg^{-1}\ K^{-1}$)	Percentage difference (%)
$Gd_5Si_{0.5}Ge_{3.5}$	60.4	52.4	–15.1
$Gd_5Si_1Ge_3$	48.1	45.7	–5.1
$Gd_5Si_{1.2}Ge_{2.8}$	46.2	43.1	–7.2
$Gd_5Si_{1.3}Ge_{2.7}$	45.2	41.8	–8.1

$Gd_5Si_{1.5}Ge_{2.5}$	43.9	39.3	–12.0
$Gd_5Si_{1.6}Ge_{2.4}$	41.0	38.0	–7.8
$Gd_5Si_{1.8}Ge_{2.2}$	39.4	35.5	–11.1
$Gd_5Si_{1.95}Ge_{2.05}$	35.0	33.6	–4.1
$Gd_5Si_{1.98}Ge_{2.02}$	37.0	33.3	–11.2
$Gd_5Si_2Ge_2$	36.4	33.0	–10.3
$Gd_5Si_{2.02}Ge_{1.98}$	32.8	32.8	−0.1
$Gd_5Si_{2.1}Ge_{1.9}$	16.0	31.8	49.8
$Gd_5Si_{2.3}Ge_{1.7}$	9.1	29.4	69.2
$Gd_5Si_3Ge_1$	8.2	21.3	61.3

Figure Captions

Fig. 1. DSC curves of $Gd_{5-x}Zr_xSi_{1.5}Ge_{2.5}$ (x = 0, 0.1).

Fig. 2. (a, b) Crystal lattices and (c–f) HEXRD patterns of $Gd_{5-x}Zr_xSi_{1.5}Ge_{2.5}$ (x = 0, 0.1) at room temperature and 200 K. Calculated patterns and their residual differences are also shown.

Fig. 3. Temperature-dependent HEXRD patterns of $Gd_{5-x}Zr_xSi_{1.5}Ge_{2.5}$ (x = 0, 0.1).

Fig. 4. Temperature dependence of lattice parameters of $Gd_{5-x}Zr_xSi_{1.5}Ge_{2.5}$ (x = 0, 0.1).

Fig. 5. Temperature dependence of bond length of crystal lattices of $Gd_{5-x}Zr_xSi_{1.5}Ge_{2.5}$ (x = 0 and 0.1).

Fig. 6. Temperature dependence of d.c. magnetization of $Gd_{5-x}Zr_xSi_{1.5}Ge_{2.5}$ (x = 0, 0.1) in magnetic fields of 0.02 T and 2 T. Insets show Curie temperatures in cooling and warming.

Fig. 7. Temperature dependence of reciprocal d.c. magnetic susceptibility (denoted as $1/\chi$) of of $Gd_{5-x}Zr_xSi_{1.5}Ge_{2.5}$ (x = 0, 0.1) in magnetic fields of (a, b) 0.02 T and (c, d) 2 T. Arrows show paramagnetic Curie temperatures in cooling and warming. Insets show onset temperatures of a Griffiths phase in cooling and warming.

Fig. 8. (a, b) Isothermal magnetization and (c) total entropy changes of $Gd_{5-x}Zr_xSi_{1.5}Ge_{2.5}$ (x = 0, 0.1) at a magnetic field change from 0 to 2 T.

Fig. 9. Schematic illustration of changes of interlayer T–T bonds of the monoclinic lattice induced by the Zr substitution.

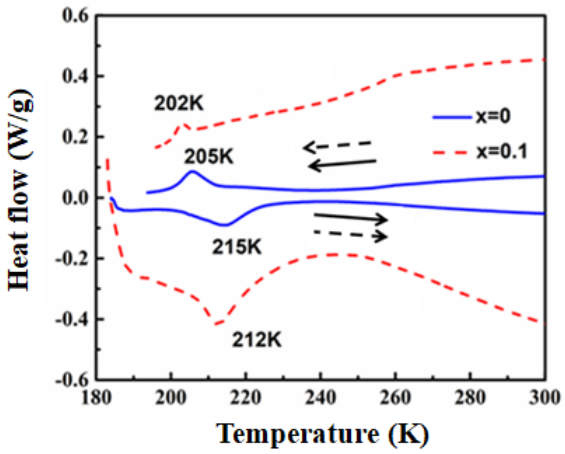

Fig. 1

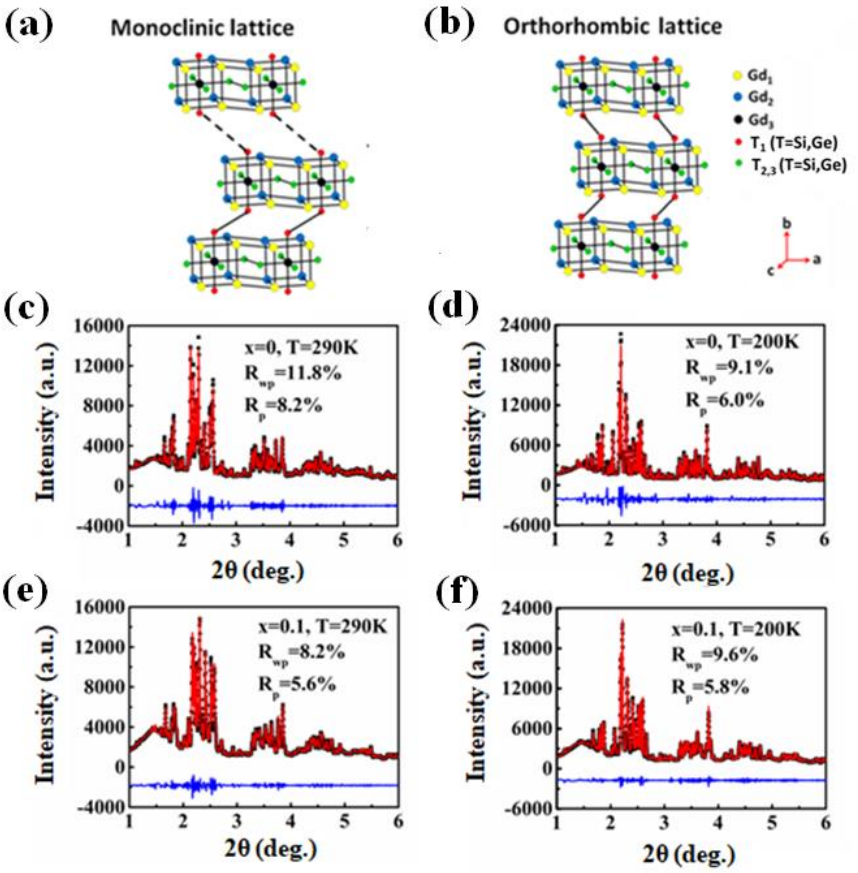
(a)
Monoclinic lattice
(b)
Orthorhombic lattice
Gd1
Gd2
Gd3
T1 (T=Si,Ge)
T2,3 (T=Si,Ge)
b
a
c
(c)
x=0, T=290K
Rwp=11.8%
Rp=8.2%
Intensity (a.u.)
2θ (deg.)
(d)
x=0, T=200K
Rwp=9.1%
Rp=6.0%
Intensity (a.u.)
2θ (deg.)
(e)
x=0.1, T=290K
Rwp=8.2%
Rp=5.6%
Intensity (a.u.)
2θ (deg.)
(f)
x=0.1, T=200K
Rwp=9.6%
Rp=5.8%
Intensity (a.u.)
2θ (deg.)

Fig. 2

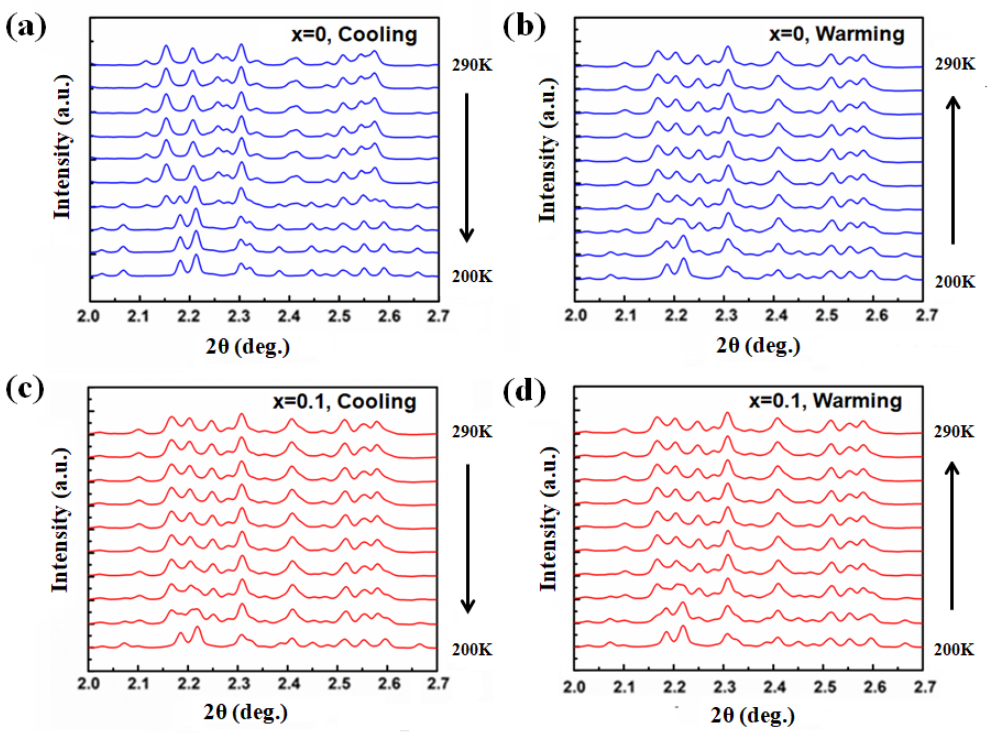
(a)
x=0, Cooling
290K
200K
Intensity (a.u.)
2θ (deg.)
(b)
x=0, Warming
290K
200K
Intensity (a.u.)
2θ (deg.)
(c)
x=0.1, Cooling
290K
200K
Intensity (a.u.)
2θ (deg.)
(d)
x=0.1, Warming
290K
200K
Intensity (a.u.)
2θ (deg.)

Fig. 3

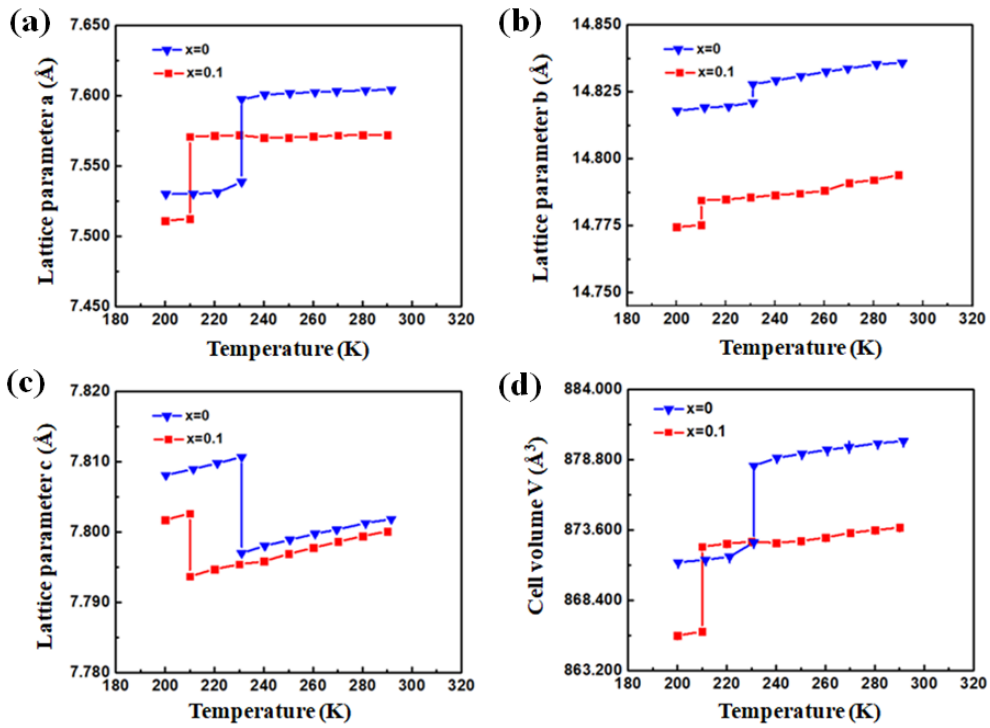
(a)
Lattice parameter a (Å)
x=0
x=0.1
Temperature (K)
(b)
Lattice parameter b (Å)
x=0
x=0.1
Temperature (K)
(c)
Lattice parameter c (Å)
x=0
x=0.1
Temperature (K)
(d)
Cell volume V (Å3)
x=0
x=0.1
Temperature (K)

Fig. 4

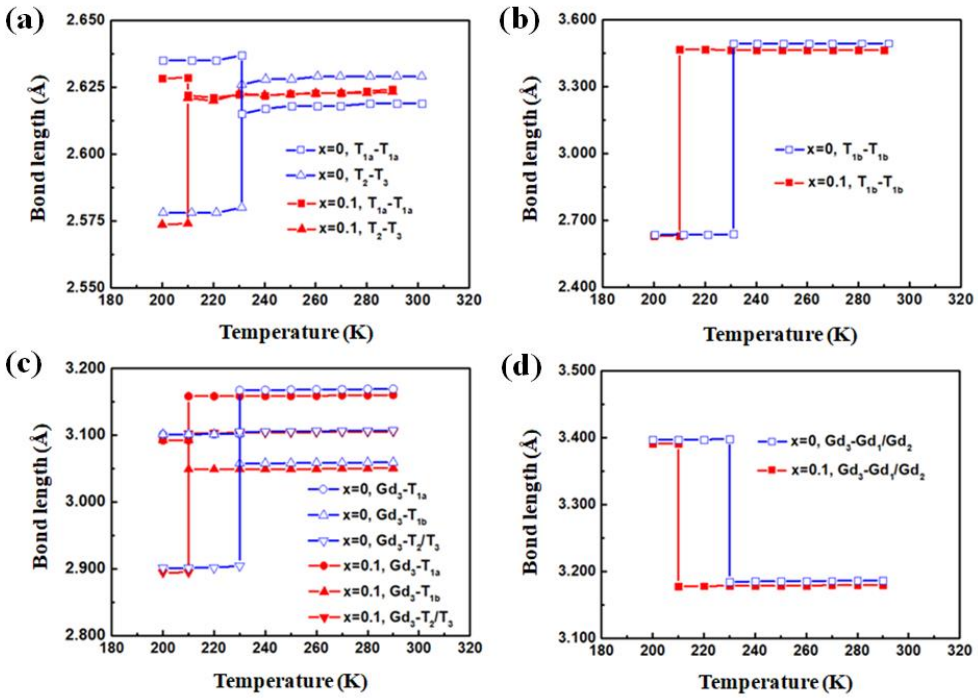
(a)
Bond length (Å)
Temperature (K)
x=0, T1a-T1a
x=0, T2-T3
x=0.1, T1a-T1a
x=0.1, T2-T3
(b)
Bond length (Å)
Temperature (K)
x=0, T1b-T1b
x=0.1, T1b-T1b
(c)
Bond length (Å)
Temperature (K)
x=0, Gd3-T1a
x=0, Gd3-T1b
x=0, Gd3-T2/T3
x=0.1, Gd3-T1a
x=0.1, Gd3-T1b
x=0.1, Gd3-T2/T3
(d)
Bond length (Å)
Temperature (K)
x=0, Gd3-Gd1/Gd2
x=0.1, Gd3-Gd1/Gd2

Fig. 5

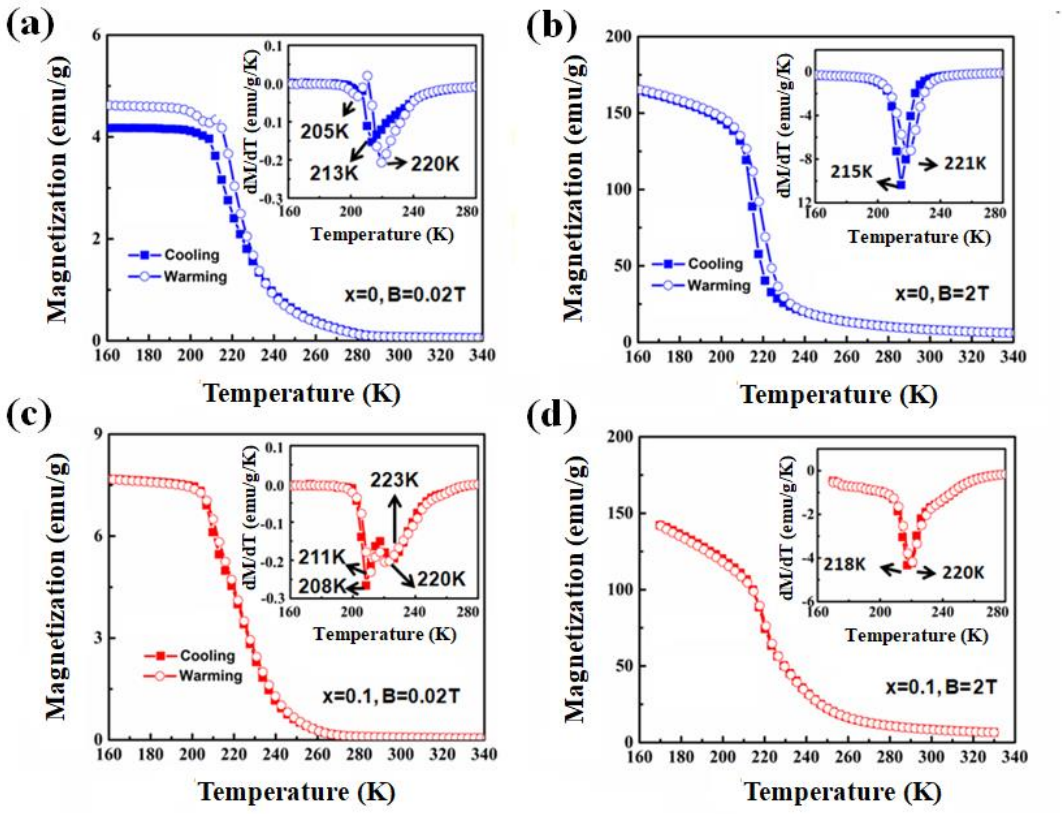
(a)
Magnetization (emu/g)
Temperature (K)
dM/dT (emu/g/K)
205K
213K
220K
Cooling
Warming
x=0, B=0.02T
(b)
Magnetization (emu/g)
Temperature (K)
dM/dT (emu/g/K)
215K
221K
Cooling
Warming
x=0, B=2T
(c)
Magnetization (emu/g)
Temperature (K)
dM/dT (emu/g/K)
223K
211K
208K
220K
Cooling
Warming
x=0.1, B=0.02T
(d)
Magnetization (emu/g)
Temperature (K)
dM/dT (emu/g/K)
218K
220K
x=0.1, B=2T

Fig. 6

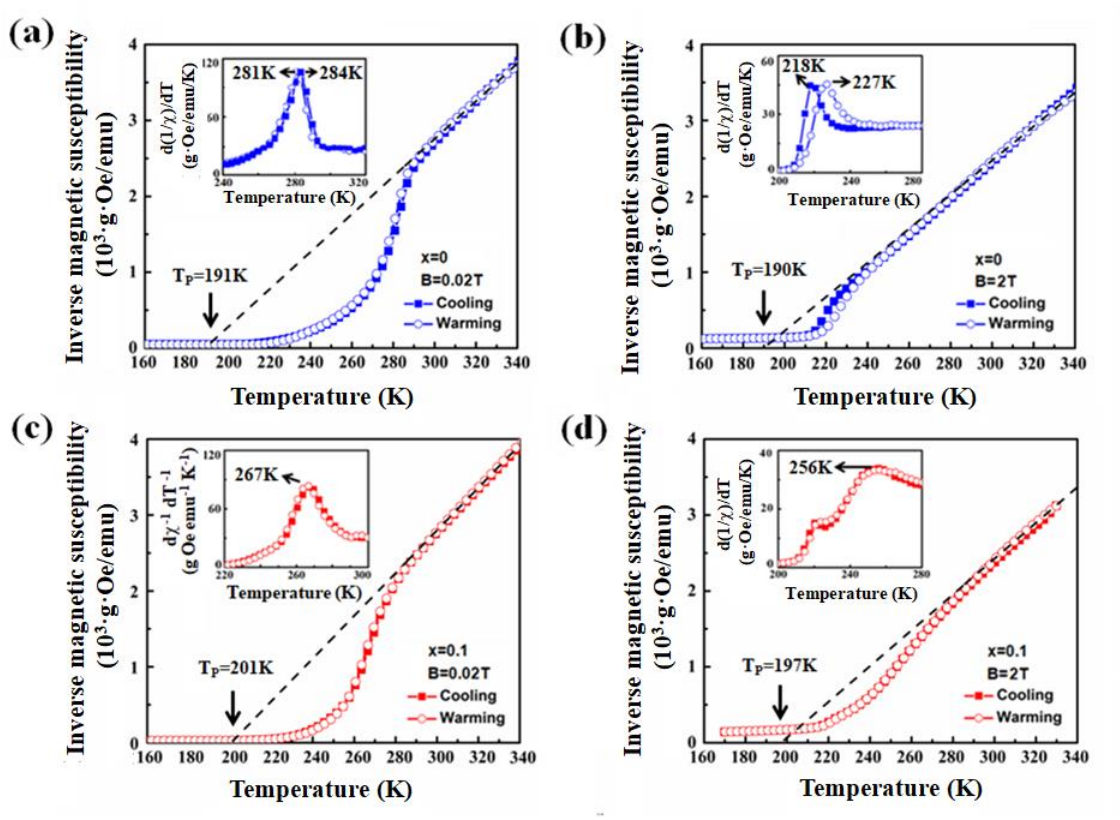
(a)
Inverse magnetic susceptibility (10³·g·Oe/emu)
Temperature (K)
d(1/χ)/dT (g·Oe/emu/K)
281K
284K
T_P=191K
x=0
B=0.02T
Cooling
Warming
(b)
218K
227K
T_P=190K
x=0
B=2T
(c)
dχ⁻¹dT⁻¹ (g Oe emu⁻¹ K⁻¹)
267K
T_P=201K
x=0.1
B=0.02T
(d)
256K
T_P=197K
x=0.1
B=2T

Fig. 7

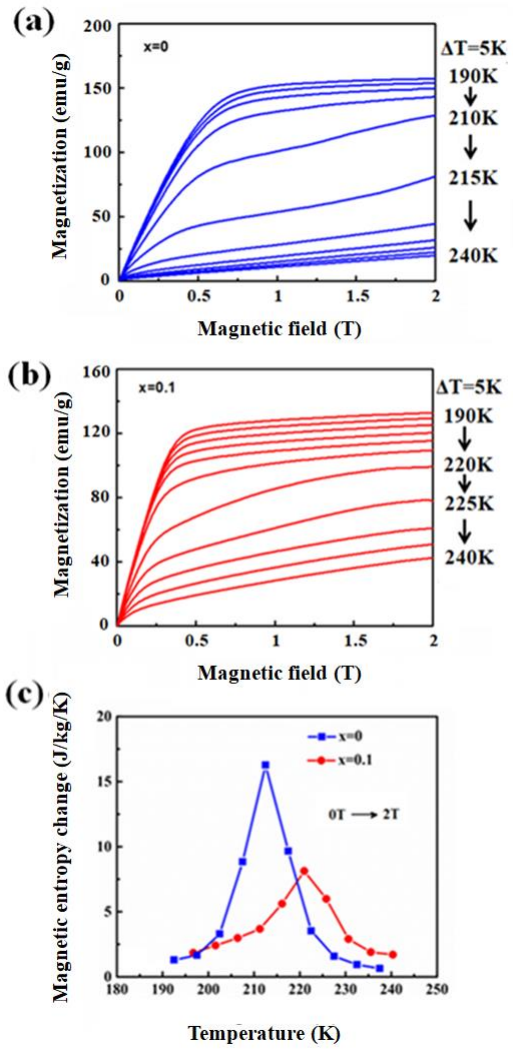
(a)
x=0
ΔT=5K
190K
210K
215K
240K
Magnetization (emu/g)
Magnetic field (T)
(b)
x=0.1
ΔT=5K
190K
220K
225K
240K
Magnetization (emu/g)
Magnetic field (T)
(c)
x=0
x=0.1
0T → 2T
Magnetic entropy change (J/kg/K)
Temperature (K)

Fig. 8